

Damage Studies of Tungsten Due To Neon Ion Irradiation

M. Bhuyan

Dept. of Physics, Rangia College, Rangia Assam, India

Abstract— Tungsten is being proposed as a front runner choice for the plasma facing component material of next generation fusion reactor because of its superior thermo-physical and mechanical properties. It is essential to study the ion material interaction for its response to severe conditions of fusion reactor. In this work, an ingenious ion source namely plasma focus is used to study the effect of neon irradiation on tungsten under various experimental conditions. Exposed and reference tungsten samples were analyzed using optical microscope, scanning electron microscope, atomic force microscope. Surface analyses confirm the formation of micro-cracks, bubbles, blisters, holes etc. X-ray diffraction pattern confirms the development of compressive stress on the sample due to thermal load and formation of other phases or some expanded phases.

I. INTRODUCTION

It is quite essential to understand the material properties in fusion environment for its better operation, safety and performance of fusion reactor. The plasma facing components (PFC) of the fusion reactor play a key role for its successful long run operation. Therefore, the behavior of different PFC materials in extreme fusion environment is of the great interest in connection with the realization of international projects ITER [1]. Tungsten is one of the most important candidates as PFC material for next generation fusion reactor because of its excellent material properties such as high melting point, high threshold energy for physical sputtering, and low retention of hydrogen isotopes [2,3]. A number of latest PF devices available for processing, thin film deposition, fabrication, implantation of ions on materials of interest are being described in our earlier paper [4]. In particular, Pimenov et al. [5] investigated the damage induced on materials that are of interest in fusion reactors namely tungsten and carbon fiber composites by using high-energy axially emitted ion beam and dense plasma streamer of a 1.2 MJ PF device. It is well known that the ion emission from the PF device is anisotropy in nature irrespective of bank energy [6] and therefore, it would be fascinating to see the effect of ion irradiation on material by keeping them not only at axial position but also at various angular positions. The studies are carried out with a view to check their strength and life time since tungsten is not only used to make material components in fusion reactor but also in vessel mirror material because of their good optical reflectivity characteristics in a wide wavelength range. Therefore, we felt that an attempt must be made in this direction so as to simulate the expected outcome of ion-

materials interaction with special scale with varied ion fluxes. In this paper, we have reported that neon ion assisted damages on tungsten samples using low energy PF device. Following section describes the experimental technique used for the studies followed by results and discussion.

II. EXPERIMENT TECHNIQUE

The schematic of the experimental setup used as neon source is shown in Fig.1. It is basically a 2.2 kJ Mather geometry PF device having powered by 7.1, 25 kV fast discharging capacitor. A homebuilt power supply is used to charge the capacitor having an inbuilt low inductance pressurized spark gap switch. The coaxial electrode system shown in Fig.1 is housed inside a stainless steel chamber of 6 litre volume. The detail descriptions of the mechanical and electrical parameters of our PF were reported elsewhere [6]. When the capacitor is discharged through the electrode system, current sheaths develop across the insulator and these sheaths are axially accelerated down the coaxial electrodes by the self-generated $J \times B$ force. At the end of the electrodes, the sheaths undergo radial pinching and forming highly dense hot plasma. This plasma is quite unstable and disrupts due to the growth of $m = 0$ instabilities, and thereby accelerating ions towards the top of the chamber and electrons towards the anode. Thus by filling the vacuum chamber with neon gas we can generate the required neon beams. High purity (99.9%) tungsten plates were procured from Goodfellow, UK. Keeping in mind the dimension of samples needed for different instrumentations (XRD, SEM, XPS etc.), square tungsten samples of sizes of 5x5 mm² and 10x10 mm² were cut from the plate with the help of precision cutter. After having required dimension of samples, they were polished using a Buehler make Minimet 1000 polisher with two steps.

First step, i.e., the rough polishing was carried out using different grits (180, 240, 360, 420, 600 and 1200) of grinding papers. The second step, i.e., the fine polishing was carried out with micro cloth using alumina reagent for half an hour and followed by nylon cloth using metadi reagent for the same time. After polishing, the roughness of the samples were gradually removed and appeared to be mirror finish. After polishing these were cleaned by putting them in ultrasonic bath. The cleaned tungsten samples of sizes of 5x5 mm² and 10x10 mm² were then introduced inside the PF chamber and mounted axially as well as at different angles with the help of a movable sample holder. The samples were exposed to the multiple PF shots (5, 10 and 20 shots) by keeping neon filling gas pressure at 0.5 Torr. The exposed and reference tungsten samples were characterized by means of different technique such as optical microscope (OM), scanning electron microscope (SEM), atomic force microscope (AFM) and grazing incidence x-ray diffraction (GIXRD) in order to ascertain the effect of impact of neon on the samples.

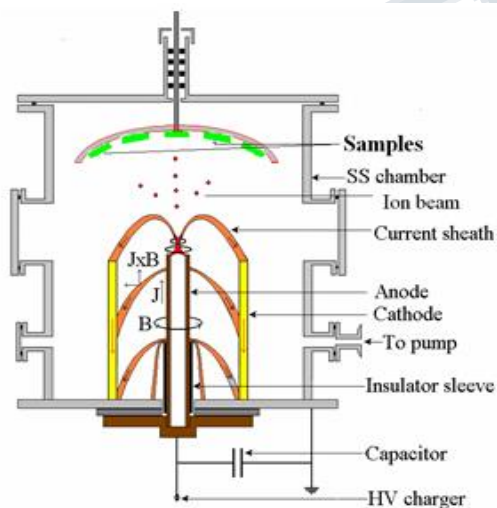


Fig. 1. Schematic diagram of the experimental setup.

III. RESULTS AND DISCUSSION

Neon ions emitted from our PF device is of the order of 1.2 MeV.[7]. After irradiation of ions on tungsten surface it started to melt the surface because of heat loading. During melting a thermo dynamical equilibrium is reached because of thermal spike and then evaporation of tungsten surface layer takes place. After exposure with our naked eye, a clear difference of the surface appearance has been observed on inspecting of the reference and ion exposed samples. The surface of the unexposed sample is light gray, smooth, and

bright looks where as the surfaces of the exposed sample are reflecting yellowish brown grey color with dull appearance. Prior to exposure and in order to know the surface morphological and microscopic damages of the surface of tungsten samples are observed using simple visualization technique i.e Olympus make OM with higher resolution (maximum 2500X). The ion fluence of the order 1018/m² with 20 PF shots were exposed to the tungsten surface and then surface deformation has been noticed in Fig.2. In Fig. 2 (a), the formation of microcrack looks like a long wave character i.e 'r' type and 'w' or wedge type cavitations are observed throughout the whole surface of tungsten. These types of formation of different cavitations are associated with thermal load or development of stress. Stress concentrations could arise at grain boundaries by several means such as presence of particles at grain boundaries, presence of irregularities, dissolved gases etc. The formation of 'r' type cavitations are associated with low stress on the other hand the formation of 'w' type cavitations with higher stresses and with sliding at triple junctions [8]. As we know that fatigue is a commonly observed form of material failure caused by cyclic loading at stresses below the yield stress. The process of fatigue failure begins with the initiation of micro cracks at various sites on the surface of the material. Some of these micro cracks eventually grow and coalesce to form larger cracks ultimately leading to fatigue failure [9]. Also in some cases cracks were found to initiate primarily in slip bands on the sample surface. Slip bands are manifestations of the dislocations along preferred plans of the atoms in the metal, which causes the material between planes to be elevated or depressed at a free surface. It is an indication that the formation of cracks result from the high residual stresses following spray processes and low strength, in particular the tensile strength [10]. Also same type of highly long micro cracks are observed on tungsten surface with deuterium ion using PF-1000 device by Pimenov et al. [5]. With long micro crack they also observed some sub branches of cracks with deuterium power density $q > 108 \text{ W/cm}^2$. These branches of crack looks like focus of lightening in their cases. Also cracks are formed because of volume defects when there is small electrostatic dissimilarity between the stacking sequences of closed packed plans. The micro-cracks also may be due to thermal shock, taking place during the ion beam incidence consisting of fast heating and strong temperature gradients [11]. In our case the width of the micro cracks vary from 5.02-11.13 μm . Along with micro cracks on some parts of irradiated tungsten surface the bubbles are observed as shown in Fig. 2(b). However once ions are implanted, the low mobility of neon in tungsten will cause them to become trapped in the metal. Neon atoms in a metal may occupy

either substitutional or interstitial sites. As interstitials, they are very mobile, but they will be trapped at lattice vacancies, impurities and vacancy-impurity complexes. With higher magnification, typical size of the bubble is of the order of 2 μm is noticed and

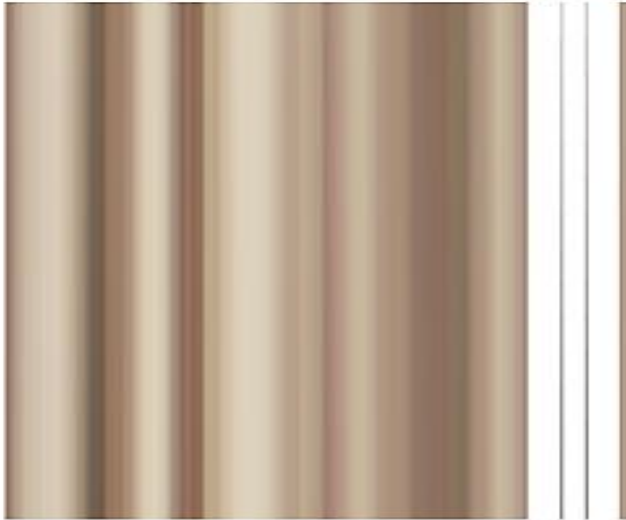


Fig. 2: Optical micrographs exhibiting the surface morphology of exposed tungsten surface for three different magnifications.

it is evident from Fig. 2(c). Bubbles of several micrometers in size are found on the surface. They are randomly distributed over the surface. Another way once implanted the neon atoms diffuse in all directions. The constant ion flux to the surface acts as a constant source in this diffusion process. Equilibrium is reached when the incident neon equals the sum of neon leaving the surface and diffusing into the substrate. Bubbles are formed due to recombination of atomic neon at defect locations. As discussed earlier appropriate arrangements were made inside the discharge chamber to keep the tungsten samples at various angular positions. It is known that the emissions of ions from PF device are anisotropy in nature and so the formations of microcracks are developed at various angular positions are expected to be different in nature. Tungsten samples subjected to ion irradiation in different angles were studied by OM. Therefore, the photographs shown in Fig. 3 are typical micrographs only in three different angular positions i.e., 0, 20 and 25°. Once the neon ions are bombarded on the tungsten samples, it seems that cracks are formed in equal space in all directions. At 0° the formation of microcracks like close loop or 'w' type cavitations are more than that of off axes. As we move to higher angles such as 20°, the close loop or 'w' type cavitations diminishes and width of

microcracks also decreases. The argument right behind this fact may be due to the development of stress is higher at axis than that of off axes. Successively at further higher angles, say at 50°, the microcracks are in the form of only 'r' type but also less i.e the development of stresses are low at 50°. The width of the micro crack is 4.41-10.51 μm at axis, which is 1.95-4.3 μm at 20° and at higher angle i.e at 50° it is 1.54-2.07 μm .

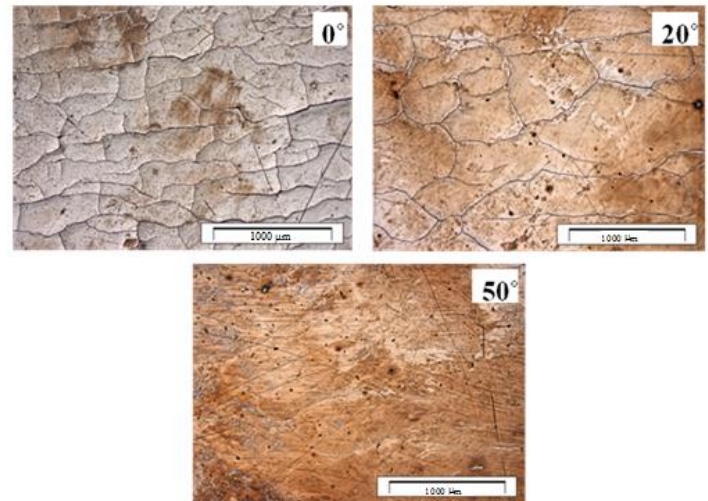


Fig. 3: Optical micrographs exhibiting the surface morphology of exposed tungsten surface for three different angular positions.

Therefore, the width of microcracks at axial position is significantly larger than at higher angles as might be expected. The most probable energy value is higher in axial position than that of] where they mentioned increase of crack width at edge part than that of central part when tungsten samples are exposed to 20 plasma pulses of 0.7 MJ/m² using plasma gun device. Quantitatively, we also estimated the number of holes and formation of 'w' type and 'r' type cavitations with respect to different angular positions. The number of holes gradually increases towards the higher angular positions, which is shown in Fig. 4. But the 'w' type cavitations decreases and at the same time 'r' type cavitations increases towards higher angular positions. It is because the developments of stresses are higher at the axis than that of off axes. As explained earlier the 'w' type cavitations are associated with higher stresses and 'r' type with lower stresses. The 'w' type or 'r' types of cavitations or microcracks are due to volumetric

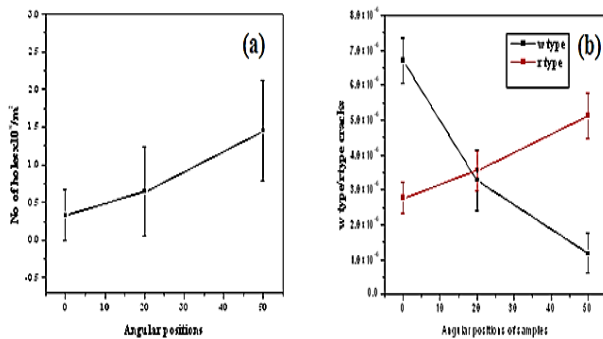


Fig. 4: Variation of number of holes (a) and number of w type/r type cracks (b) with respect to angular positions.

and numbers of holes or pores are due to interstitial defects. These type of formation stem up as a result of defects. An interstitial defect result is generally created when a foreign substitute replaces a parent atom in the lattice. This impurity is a small size foreign atom occupying an interstice or space between the regularly position, it also can be termed as vacancy in between two atomic levels. These types of holes are also created on the tungsten surface when irradiated by high density plasma [13]. Cipiti et al. noticed different sizes of pores on tungsten with the deuterium of total fluence $2 \times 10^{18}/m^2$ [14]. At axis the formation of microcracks are more means number of holes are less but at off axes formation of microcracks are less that means the numbers of holes are always trying to form a long path cracks. Scanning electron micrographs (SEM) are taken to observe the surface morphology changes using SEM of JSM-6360 (JEOL) make. The magnification of this model varies from 8x to 300000x with secondary electron image mode (SEI) to verify all these damages with higher magnifying scale. SEM images of tungsten sample exposed to neon ion are shown in Fig.5. Fig. 5(a) shows formation of cracks as a result of thermal load or development of stresses [15]. The size of micro crack of $\sim 2 \mu m$ is shown in (a). In Fig.5 (b), the holes of maximum size $5 \mu m$ is distinctly observed. Similarly pinholes with a size of about $0.1 \mu m$ in waved structures were observed for Ne⁺ implantation by Shu et al. [16]. Due to interstitial defects or dislocation of the particle, after the implantation of the ions, the holes/pores may occur. Formation of bubbles is also seen in Fig. 5 (c). The formation of bubble is occurred due to the trapping of neon atoms to thermal vacancies on the surface of the tungsten. Also one may explain that intrinsic defects have a little effect on the bubble formation. The bubble size is approximately $1 \mu m$ as shown in



Fig. 5: Surface morphology of exposed tungsten surface as observed under SEM depicting (a) cracks, (b) holes, (c) bubbles and (d) blister.

Fig.5(c). Similarly sparse population of small bubble approximately $1-3 \mu m$ in diameter is reported by Venhaus et al. [17]. This type of formation on the tungsten surface is also reported by Ohno et al. [3]. They irradiated the tungsten sample with deuterium plasma at 550K subsequent to the helium plasma pre-exposure at 1600K. The helium bubbles formed along the grain boundary could make grain ejection much easier. With higher magnification the size of the bubbles is $\sim 1 \mu m$. Blister like structure has been shown in Fig. 5(d). The size of the blister is $2-2.5 \mu m$ in diameter. One of the reasons for the blister formation in metals is agglomeration of the implanted gas atoms [18]. The implanted neon will also diffuse in all directions in tungsten and trapped dominantly at intrinsic vacancies as well as at grain boundaries. Neon forms gas bubbles in tungsten, where the bubbles grow by ejecting tungsten atoms from their lattice site as more neon atoms reach the site. When gas bubbles are formed in tungsten, they finally lead to a large blister formation due to high gas pressure, which is confirmed, from Fig. 5(d). Haasz et al. [19] reported blisters $10-50 \mu m$ in diameter on tungsten sample exposed to 500 eV deuterium ions having a fluence of $>10^{20} D^+ /cm^2$ at 500K. Simple Bragg diffraction did not provide any prominent differences of XRD pattern between unexposed and exposed samples. Micron sizes crack formation from surface morphology study indicates that the structural changes occur only on the near surface layers. Therefore we employed GIXRD spectrometer to obtain information on near surface structural changes. GIXRD analysis was carried out using SEIFERT XRD 3000PTS model with $CuK\alpha = 0.15406 nm$ radiation source which was operated at 40kV and 50mA. The tungsten specimen is crystal (bcc) with ductility properties.

The GIXR diffractogram of the unexposed sample is shown in Fig.6, where four peaks with planes (110), (200), (211) and (220) are clearly noticed. The GIXR diffractogram of the neon ion exposed samples with 20 PF shots are also shown in the same figure. After exposure new planes such as (111), (311) and (220) are clearly observed from the diffractograms.

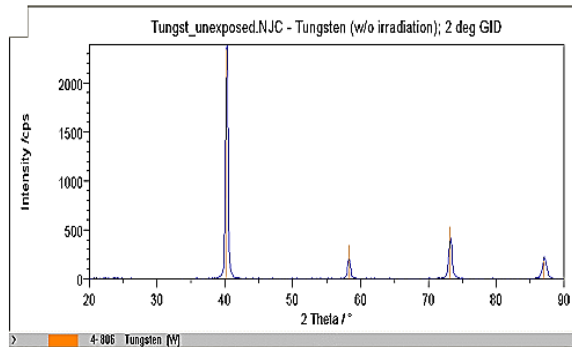


Fig. 6: GIXRD patterns of reference (top) and exposed samples (bottom).

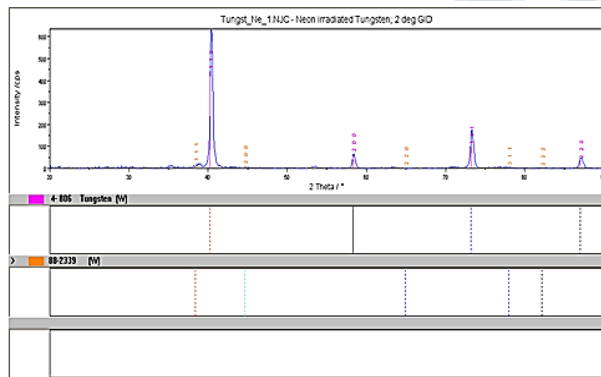


Fig. 6: GIXRD patterns of reference (top) and exposed samples (bottom).

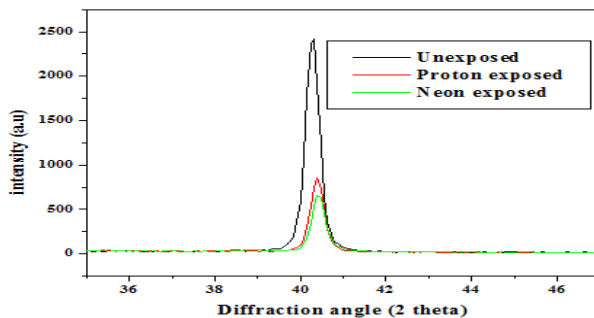


Fig. 7: GIXRD pattern of most intense peak.

It is noticed from Fig.7 that there is a small shifting of the spectrum towards the higher angular side in case of exposed

samples than that of the reference sample.

IV. CONCLUSION

The neon assisted damage studies in tungsten –a PFC component of next generation fusion reactor are carried out successfully by employing various instruments such as OM, SEM, AFM and GIXRD. Surface morphology studies reveal the various types of deformation such as microcracks, holes, bubbles, large blister, melting, defects, etc on the material surfaces due to neon beams irradiation. The formation of microcracks emerges like ‘r’ and ‘w’ type cavitations throughout the exposed surface that is seen to depend upon both angular positions as well as number of PF shots. It thermal load developed due to ion irradiation is seems to be associated with the formation of different type of cavitations. Quantatively, we have observed that the number of holes gradually increases for samples kept toward the higher angular positions and with higher number of PF shots. Complementally, ‘w’ type cavitations decreases and ‘r’ type cavitations increases for the samples kept toward the higher angular positions as well as with higher PF shots. SEM micrographs confirm the development of microcracks, holes, bubbles, blisters, localized heating, etc. In comparison to reference sample which is fairly smooth appearance, the surface morphology of the exposed sample some bubbles like structure of the order of about 100 nm size has noticed distinctly. Structural analyses using GIXRD confirms the development of compressive stress on tungsten surface due to neon ions irradiation. Diffractograms reveal the structural transformation occurred in tungsten upon irradiation and thus developing some other phases or some expanded phases.

REFERENCES

- [1] W. B. Gauster, W. R. Spears, ITER Joint Central Team, Nucl. Fusion 5 (1994) 7.
- [2] Lawrence Livermore National Laboratory (1992) Inertial Confinement Fusion, In ICF Annual Report, 1 (1991).
- [3] N. Ohno, S. Kajita, D. Nishijima, S. Takamura, J. Nucl. Mater. 363 (2007)1153.
- [4] M. Bhuyan, S.R. Mohanty, C.V.S. Rao, P. A. Rayjada, P. M. Raole, Appl. Surf. Sc, 264(2013)674
- [5] V. N. Pimenov, E. V. Demina, S.A. Maslyaev, L.I. Ivanov, V.A. Gribkov, A.V. Dubrovsky, U. Ugaste, T. Lass, M. Scholz, R. Miklaszewski, B. Kolman, A. Tartari,

Nukleonika 53 (2008)111-121

[6] S. R. Mohanty, H. Bhuyan, N. K. Neog, R. K. Rout, E. Hotta, Japan. J. Appl. Phys. 44 (2005) 5199.

[7] M. Bhuyan, N. K. Neog, S. R. Mohanty, C. V. S. Rao and P. M. Raole, Phys. of Plasma 18, 033101 (2011)

[8] B. B. Cipiti and G. L. Kulcinski, J. Nucl. Mater., 347 (2005) 298

[9] B.Riccardi,A. Pizzuto, L.Bertamini,M.Diotallevi and G.Vieider, Proc of the SOFE, 17 910 (1997)

[10] H.Iwakiri, K. Yasunaga, K.Morishita and N.Yoshida,J.Nucl. Mater.,283 1134 (2000)

[11] G.Sanchez and J. Feugeas, J.Phys.D:Appl.Phys., 30 ,927 (1997)

[12] Y. Kikuchi et al., J. Nucl. Mater. 415 (2011) 55.

[13] S.Takamura,T.Miyamoto,Y.tomida,T.Minagawa and N.Ohno,J.Nucl.Mater.(2011)

[14] W.D. Nix and J.C. Gibeling, Flow and Frature at Elevated Temperatures 7 (ASM, 1985)

[15] V.A. Gribkov et al. , Ieee Trans Plasma Sci.,30 3 (2002)

[16] W.H. Shu et al., J.Nucl.Mater., 390,1017(2009)

[17] T. Venhaus, R. Causey, R. Doerner, T. Abeln, J. Nucl. Mater. 290 (2001) 505.

[18] K.Tokunaga et al.,J.Nucl.Mater.337 887 (2005)

[19] A.A. Haasz, M.Poon and J.W. Davis, J.Nucl.Mater. 266 52 (1999)